

sPHENIX MVTX Pixel Detector Internal Alignment with AI-ML Approach

Jaehyun Kim for the sPHENIX Collaboration

Department of Physics, Yonsei University, Seoul, Korea



Abstract

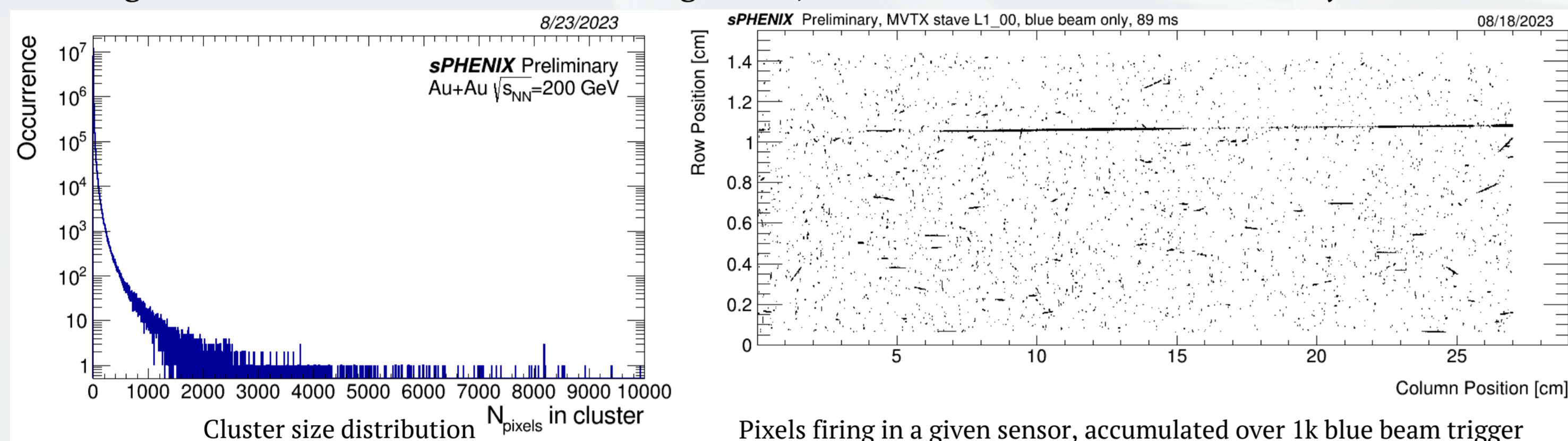
The sPHENIX experiment has achieved a major milestone with the construction and installation of the cutting-edge three-layer Monolithic-Active-Pixel-Sensor (MAPS) based VerTeX detector (MVTX) in April 2023. The sPHENIX beam commissioning was carried out with Au+Au collisions in June 2023. The MVTX is the innermost tracking detector, boasting a remarkable spatial resolution of 5 μm and covering 2.5-4.0 cm radially and a pseudo rapidity range of $|\eta| < 2$. With 432 ALPIDE sensors, each containing approximately 0.5M 27 μm x 29 μm pixels in an area of 1.5cm x 3.0cm, determining the position of each pixel in the sPHENIX global coordinate system presents a significant challenge. Our first step is to establish the relative position of each sensor in the local MVTX coordinates with an accuracy of better than 5 μm .

To this end, we have developed an AI-ML-based approach to determine the deviations of each sensor's position and orientation from the ideal geometry (dx , dy , dz) in translation and ($d\alpha$, $d\beta$, $d\gamma$) in rotation. In this presentation, we verify the successful operation of the MVTX detector in the commissioning stage and report the current status for the internal alignment.

Cluster Characteristics

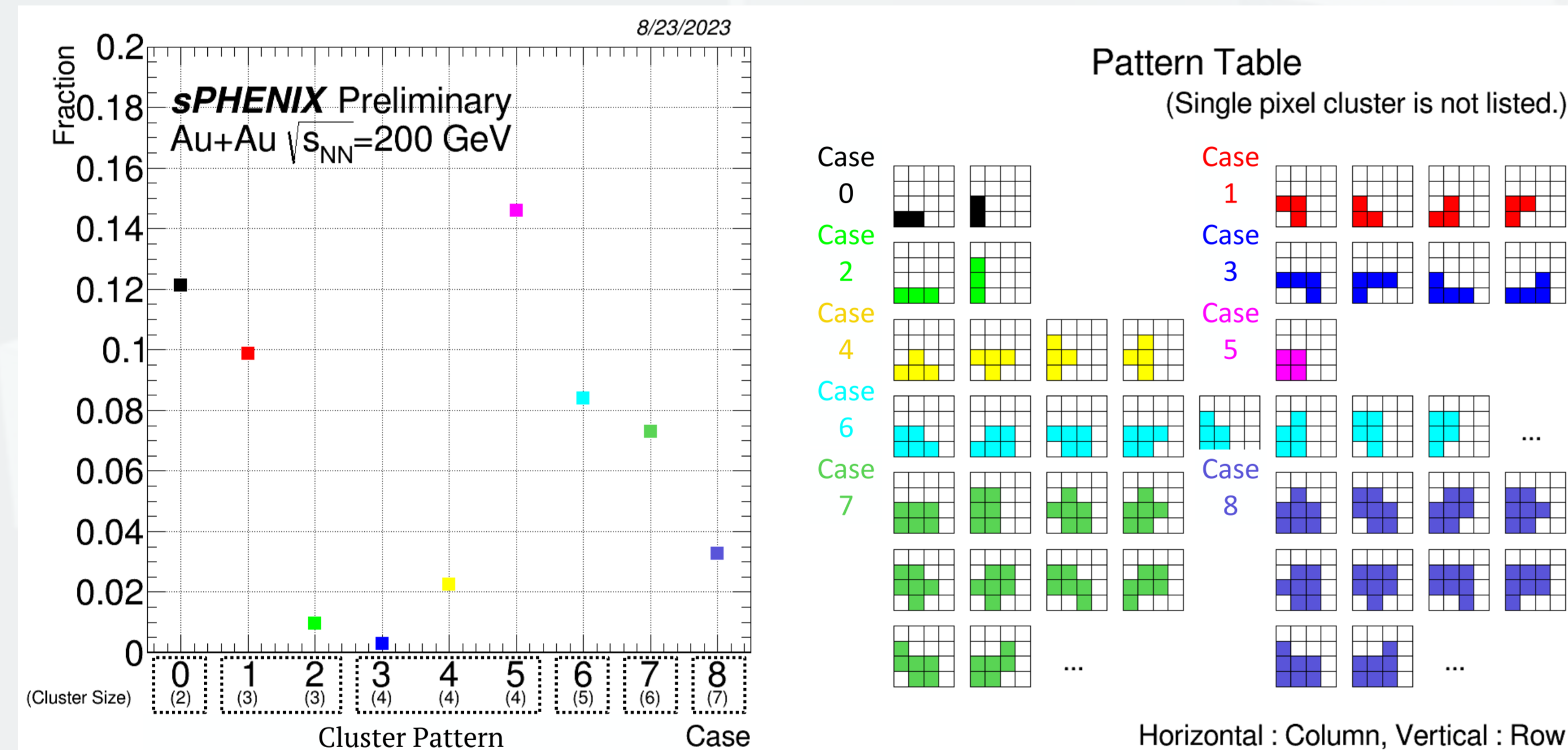
A highly energetic charged particle usually creates a cluster, a few consecutively firing pixels, in a detector layer, which has been confirmed in the test beam data. We define the size of each cluster, N_{pixels} , as the number of pixels associated to the cluster.

1. Significant number of clusters have large sizes, different from the test beam study.

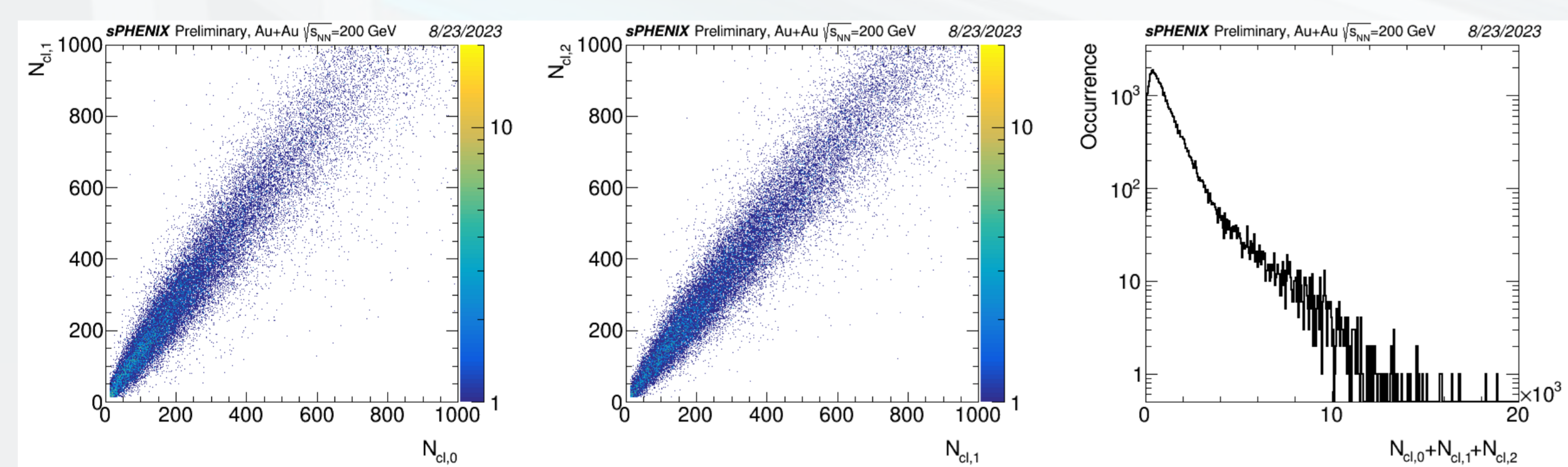


The MVTX group has been working closely with CA-D to understand and improve the beam conditions. During the initial stage of commissioning, notably large clusters were detected, which were ascribed to unanticipated high backgrounds related to the beam.

2. Most frequent cluster patterns have 4 or less pixels firing.



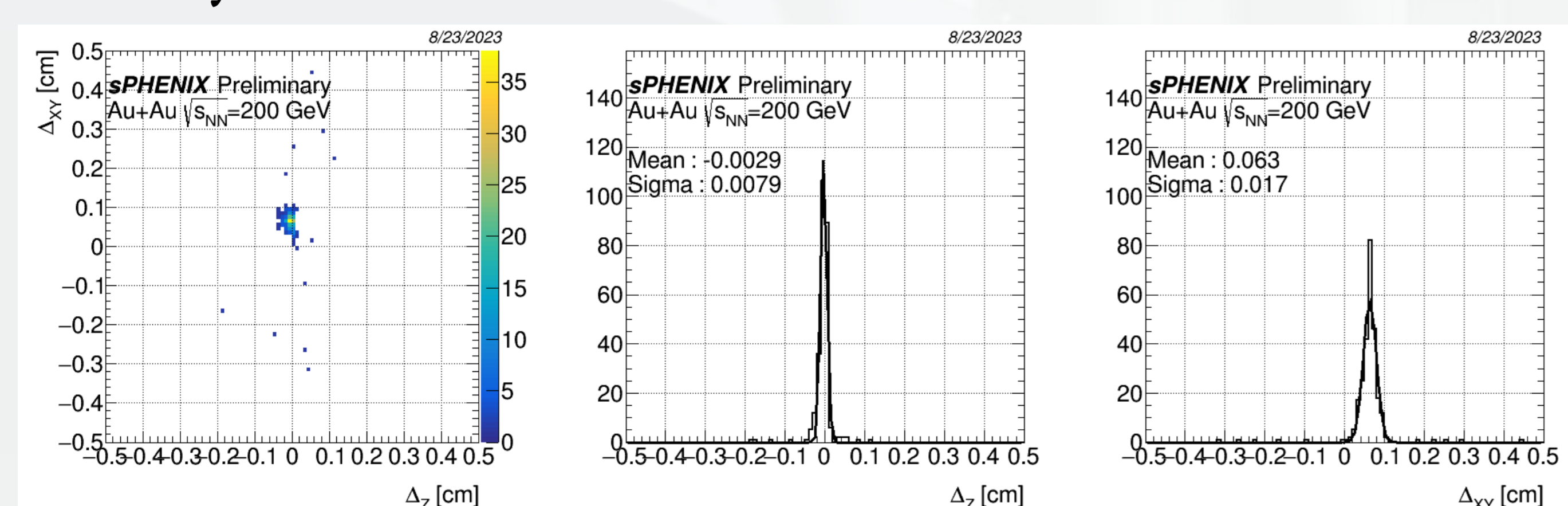
The typical cluster patterns are similar to the one of the previous application (The ITS2 upgrade of the ALICE experiment) and the test beam data. These patterns are used to define the normal clusters corresponding to about 55% of the whole clusters. The global position of the normal cluster is calculated from the associated pixel positions by arithmetic mean.



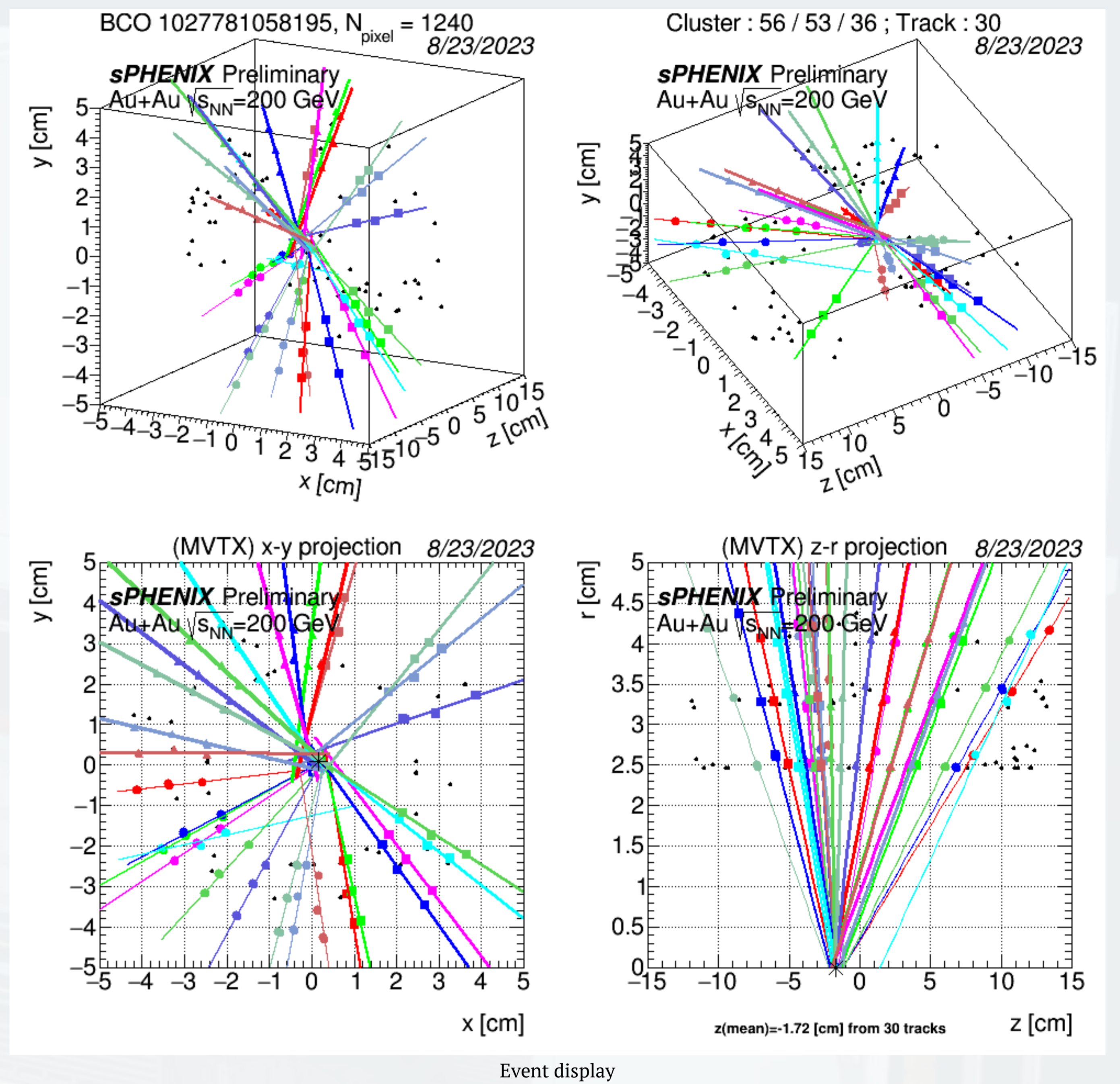
Distributions of the normal cluster numbers in the layer 0, 1, and 2 per ROF, $N_{cl,0}$, $N_{cl,1}$, and $N_{cl,2}$

The MVTX detector has read out continuously at 11kHz. Approximately 50% of the readout frames (ROFs) have small numbers, specifically 12, of normal clusters in the layer 0, 1, and 2. These frames are classified as silent and not containing real collisions. Plots above are from the remaining 50%, most of which will also not contain real collisions considering the collision trigger rate. The number of clusters in the layer 0, 1, and 2 show a good correlation though.

Summary and Outlook



Crude Tracking & Event Display



We scanned 100,000 ROFs (~1000 Zero Degree Calorimeter coincidence) from the RUN 20124 and reconstructed the particle trajectories.

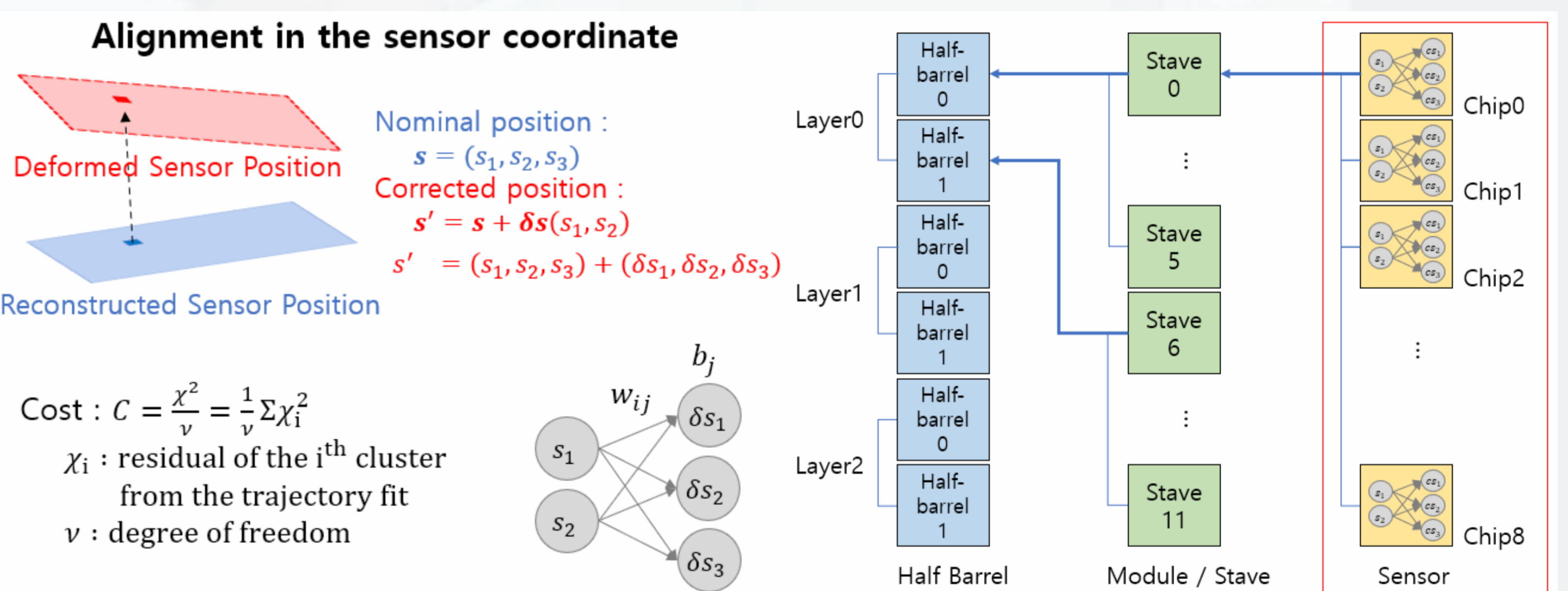
We assumed

- three consecutive hits in the layer 0, 1, and 2 tolerating loss of trajectories in favor of clarity, and
- there are approximate detector alignments,
- particle trajectories are straight within the given limitation,
- and collisions occurred along the nominal collision axis allowing sufficiently large search window.

We selected low occupancy ROFs ($N_{cl,2} < 50$) to contain peripheral collisions, and ensure sufficient granularity to verify the coincidence of hits.

Alignment with AI-ML Approach

Alignment parameter : ($\tau_1, \tau_2, \tau_3, \alpha, \beta, \gamma$)



With the linearized activation function,

Neuron output bias (b_1, b_2, b_3)

→ Translation : (τ_1, τ_2, τ_3)

Synapse weights ($w_{11}, w_{12}, w_{13}, w_{21}, w_{22}, w_{23}$)

→ Rotation : Euler angle (α, β, γ)

A system for the detector alignment based on Artificial Intelligence - Machine Learning approach is ready. Decent amount of high purity particle trajectory samples will trigger the application.

We performed a quick diagnostics to verify 267 trajectories found from 12 selected events. The above figure shows the distribution of deviations Δ_Z and Δ_{XY} from the straight-line assumption, defined as shown using the nominal position (x_L, y_L, z_L) of the clusters in the layer $L = 0, 1$, and 2.

$$\Delta_Z = z_{1,projected} - z_1 \text{ and } \Delta_{XY} = \phi_{1,projected} \sqrt{x_{1,projected}^2 + y_{1,projected}^2} - \phi_1 \sqrt{x_1^2 + y_1^2}$$

While the distribution of Δ_Z is centered around zero with the spread of about 80 μm , the one of Δ_{XY} has a peak with the spread of about 170 μm at an offset of about 630 μm . Generous search window for the coincident hits appears with large tails. Considering the used cluster positions are derived from 'nominal pixel position', this small offset might be attributed to the misalignment among the detector layers, and wider spread of the peak in the same distribution can be due to the deflection of the particle trajectories in the magnetic field or misalignment along azimuth direction. We are ready to initiate the first stage of the alignment process while extending the analyzed event class (centrality).